A Phase-Sensitive Detection Method Using Diffractive Optics for Polarization-Selective Femtosecond Raman Spectroscopy

M. Khalil, N. Demirdöven, Oleg Golonzka, C. J. Fecko, and A. Tokmakoff*

Department of Chemistry, Massachusetts Institute of Technology, Cambridge, Massachusetts 02139

Received: December 22, 1999; In Final Form: April 5, 2000

A phase-sensitive detection method that uses two diffractive optics for femtosecond nonresonant Raman spectroscopy is demonstrated. One diffractive optic is used for generating the three input pulses for the third-order nonlinear experiment, and the second is used for recombining the signal with a passively phase-locked local oscillator derived from the probe pulse. This approach allows for phase-sensitive detection, direct phase calibration, control over all field polarizations, and removal of unwanted two-pulse signal contributions. Experiments on the intermolecular dynamics of CS_2 and CH_3CN demonstrate that the birefringent (in-quadrature) signal amplitude is significantly greater than the dichroic (in-phase) contribution. Polarization-selective measurements are used to project the isotropic birefringent response for CS_2, which suppresses reorientational dynamics and allows interaction-induced effects to be observed.

Introduction

Advances in the study of condensed-phase dynamics through nonlinear spectroscopies have largely occurred through improvements in time-resolution and frequency tuning range of pulsed laser sources. In recent years there has been an increased need for expanding the control of phase in coherent spectroscopies, both for the input fields and for phase-sensitive detection of coherent signals. While phase control over input fields is the basis for many coherent control experiments,[1] phase-sensitive detection is important for describing the trajectories of ground- and excited-state wave packets,[2] for probing solvation dynamics,[3] and for developing coherent two-dimensional spectroscopy.[4,5] More generally, control over phase both in the input and in the detection is of interest for developing optical NMR analogues, from coherent multipulse experimental methods to phase cycling in data acquisition.

In this paper, we demonstrate a phase-sensitive detection method for nonresonant femtosecond (fs) Raman experiments that can be used for polarization-selective nonlinear spectroscopy. Phase-sensitive detection for fs nonresonant experiments on liquids and solutions was originally developed using optical-heterodyne-detected optical Kerr effect (OHD−OKE) spectroscopy[6−9] as a method of measuring transient birefringence and transient dichroism.[10−13] Since detection schemes employing a square-law detector are insensitive to the phase of the signal field, the technique of optical heterodyne detection (OHD)[14] is used where phase-sensitive detection is required. A weak signal is mixed with a strong reference field, or local oscillator (LO), and the interference between the two fields is detected. In OHD−OKE pump−probe spectroscopy, the signal is generated collinear to the probe pulse, so that the probe pulse acts as an intrinsic LO to the signal. Though a powerful method, OKE−OHD is fundamentally limited by lack of polarization control; it can measure only the pump-induced anisotropy dynamics.

The need to have control over the polarizations of all fields in third-order nonlinear spectroscopies led to developments of several new extensions of nonresonant transient-grating (TG) methods to include the detection of signals with OHD schemes. Using a high-repetition rate system, a thermal grating has been used as a LO for the nuclear response,[15] allowing no control over the LO field. Local oscillators have also been mixed with TG signals after the sample in an unstabilized manner[16] and by using an actively phase-stabilized Mach−Zender interferometer.[17] Even when actively stabilized, phase drift between the signal and LO has been unavoidable. Recently, the use of diffractive optics (DO) as a method of generating passively phase-locked pulse pairs for heterodyne-detected nonresonant spectroscopy has been demonstrated by Miller and co-workers[18,19] and Nelson and co-workers.[20,21] A DO is a transmission grating that is used to generate +1 and −1 diffraction orders of equal intensity. These pulses are then imaged as a pair onto a sample. Since both beams are imaged with the same optics, no beam splitter exists and the pulse pair is phase locked. Previous work with DOs has demonstrated that two pulse pairs, produced by the same DO, can be used to generate a three-pulse TG signal, which emerges collinear with the fourth field.[18,19,21] The fourth pulse acts as a passively phase-locked LO and can be used for phase-sensitive OHD. Here we present a new approach of using two DOs to generate and detect nonresonant fs Raman signals in a phase-sensitive manner to distinguish between the in-phase (dichroic) and in-quadrature (birefringent) signal contributions. We demonstrate the ability to unambiguously suppress additional signal contributions that are generated in the same phase-matched direction. In addition, unwanted signal contributions can be removed by cycling the phase of the local oscillator. The TG method also allows independent control over the polarization of the input beams and of the detected signal, to measure any component of the fourth-rank polarizability tensor.

The fs nonresonant Raman pulse sequence is shown in Figure 1(a). Two nonelectronically resonant pump pulses impulsively create a vibrational coherence which propagates until a probe, delayed by time τ, stimulates the emission of the nonlinear signal into the $\mathbf{k_s} = \mathbf{k_1} - \mathbf{k_2} + \mathbf{k_3}$ wave vector matching direction.

* E-mail: tokmakof@mit.edu. Fax: 617-253-7030.

10.1021/jp994455q CCC: $19.00
Published on Web 05/20/2000

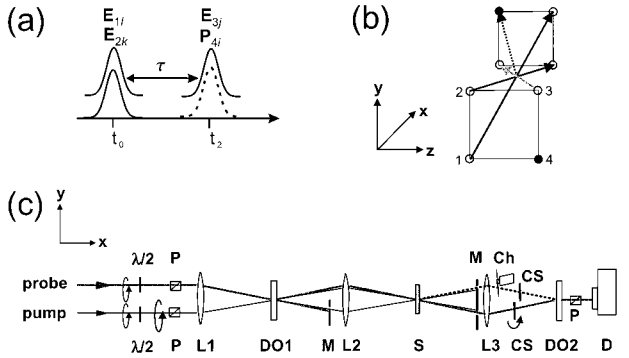

Figure 1. (a) Time variables in the third-order fs Raman experiment where the subscripts $i-l$ refer to the polarization of the beams. Beams 1 and 2 are the pump pulses, and 3 and 4 are the probe and the signal field generated by the third-order polarization, respectively. (b) "Boxcar" phase matching geometry of the TG experiment. The three input beams are incident along $\mathbf{k_1}$, $\mathbf{k_2}$, and $\mathbf{k_3}$ and the TG signal is generated along $\mathbf{k_4}$. (c) Dual-diffractive-optic experimental schematic for phase-sensitive detection of TG experiment separating the pump−probe signals from the TG signal: $\lambda/2$, half-wave plate; P, polarizer; L, lens; DO, diffractive optic; S, sample; M, mask; Ch, chopper; CS, cover slips, and D, detector. Note that the actual experiment uses all-reflective optics where L2 and L3 represent a concave imaging mirror and a flat folding mirror.

The response of a liquid to impulsive nonresonant Raman excitation is described by a two-point polarizability correlation function of the form[22]

$$R^{(3)}_{ijkl}(\tau) = \langle[\alpha_{ij}(\tau),\alpha_{kl}(0)]\rangle \tag{1}$$

The indices i, j, k, and l, which represent field polarizations, refer to the laboratory-frame coordinates over which the molecular polarizability is ensemble-averaged to obtain the tensorial response function. Independent measurement of these tensor elements through polarization-selective experiments allows the separation of nuclear motions by their symmetry properties. Polarization selectivity proves to be an important tool for understanding condensed-phase dynamics. For a nonresonant experiment on an isotropic liquid, measurements of the isotropic and anisotropic response functions completely describe the polarizability relaxation dynamics and allow us to separate the time scales of the isotropic vibrational dynamics and reorientational motions. For high-frequency vibrations, the isotropic response function (R_{ISO}) observes the dephasing without contributions from orientational relaxation.[23] For the study of collective liquid motions, R_{ISO} suppresses librational and other reorientational motion and is thus a direct and sensitive method for probing interaction-induced effects in liquids. We demonstrate this ability by measuring the isotropic birefringent polarizability relaxation dynamics in CS_2.

The third-order macroscopic polarization, $\mathbf{P}^{(3)}(\tau)$ is obtained by convolution of $\mathbf{R}^{(3)}(\tau)$ over the input fields. It can be expressed as a sum of cosine and sine terms[12]

$$\begin{aligned}\mathbf{P}^{(3)}(\tau) &= P^{(3)}(\tau)e^{-i\omega\tau} + [P^{(3)}(\tau)]^* e^{i\omega\tau} \\ &= 2\mathrm{Re}[P^{(3)}(\tau)]\cos(\omega\tau) + 2\mathrm{Im}[P^{(3)}(\tau)]\sin(\omega\tau)\end{aligned} \tag{2}$$

$P^{(3)}$ is the complex scalar amplitude oscillating at the center frequency ω of the pump and probe pulses. Radiation of the signal field by the third-order polarization leads to a $\pi/2$ phase shift. This allows us to express the signal as a sum of two contributions: the birefringent (E_{bir}) and dichroic (E_{dic}) responses.

$$\begin{aligned}\mathbf{E}_S(\tau) &= \frac{i2\pi\omega l}{nc}\mathbf{P}^{(3)}(\tau) \\ &= \frac{2\pi\omega l}{nc}(2\mathrm{Re}[P^{(3)}(\tau)]\sin(\omega\tau) + 2\mathrm{Im}[P^{(3)}(\tau)]\cos(\omega\tau)) \\ &= E_{bir}(\tau)\sin(\omega\tau) + E_{dic}(\tau)\cos(\omega\tau)\end{aligned} \tag{3}$$

The birefringent response corresponds to the real part of the nonlinear polarization and represents the phase shift (retardance) of the signal field induced by the sample, whereas the dichroic response, or imaginary part of the nonlinear polarization, describes the sample-induced amplitude variation in the signal field. Moreover, dynamics observed in the dichroic and birefringent responses can be helpful in separating signal contributions from excited and ground states, respectively.

A typical OHD scheme coherently mixes a strong reference field, the local oscillator $\mathbf{E}_{LO}(\tau)$, with the weak signal field, $\mathbf{E}_S(\tau)$. Let us represent the LO as

$$\mathbf{E}_{LO}(\tau,\phi) = \mathbf{E}_{LO}(\tau)\cos(\omega\tau + \phi) \tag{4}$$

where ϕ is the phase of the LO with respect to the signal field. The detector sees the sum of the LO field and the signal field generated by $\mathbf{P}^{(3)}(\tau)$.

$$I(\tau,\phi) = \frac{nc}{4\pi}|\mathbf{E}_{LO}(\tau) + \mathbf{E}_S(\tau)|^2 \tag{5}$$

By chopping $\mathbf{E}_S(\tau)$, the homodyne contribution from the LO is eliminated in the limit that that $\mathbf{E}_{LO} \gg E_{bir}, E_{dic}$.

$$\begin{aligned}\mathrm{I}(\tau,\phi) &= \frac{nc}{4\pi}[|\mathbf{E}_{LO}(\tau)\cos(\omega\tau + \phi) + E_{bir}(t)\sin(\omega\tau) + \\ &\qquad E_{dic}(\tau)\cos(\omega\tau)|^2 - |\mathbf{E}_{LO}(t)\cos(\omega\tau + \phi)|^2] \\ &\approx \frac{nc}{2\pi}[\mathbf{E}_{LO}(\tau)E_{bir}(\tau)\sin(\phi) + \mathbf{E}_{LO}(\tau)E_{dic}(\tau)\cos(\phi)]\end{aligned} \tag{6}$$

It is clear from the above equations that we can selectively observe the birefringent ($\phi = \pi/2, 3\pi/2...$) and dichroic ($\phi = 0, \pi...$) response of the molecular system by controlling the relative phase of the LO with respect to the signal field. Note that the detected signal is amplified by a factor of $2|\mathrm{ELO}|/|\mathrm{ES}|$ in this phase-sensitive technique in comparison to a homodyne detection scheme, which proves to be advantageous when the signal of interest is very weak.

Experimental Section

Phase-sensitive femtosecond nonresonant Raman measurements were performed with 50 fs pulses at 650 nm derived from an optical parametric amplifier pumped by a 1 kHz Ti:sapphire regenerative amplifier. The 800 nm, 100 fs fundamental pulses were parametrically down converted into signal and idler pulses in a 1 mm type II BBO crystal. Visible pulses were obtained by frequency doubling the 1.3 μm idler pulses in a 1 mm type I BBO crystal. Autocorrelations were performed on the 650 nm pulses following prism pair compensation for positive group velocity dispersion (GVD) originating from the optical materials used in the experiment. Intensity autocorrelations of the compensated pulses were well fit over >2 decades in intensity by assuming a 50 fs pulse with a Gaussian temporal profile. This results in a time bandwidth product of <0.5.

Following a beam-collimating telescope and the prism pair, the pulse train was split into two beams for the pump and the probe arm. The probe was delayed with respect to the pump by

using a stepper motor with 0.1 μm resolution. Each arm contained a half-wave plate followed by a polarizer, allowing both the polarization and pulse intensity to be controlled for each pulse. The interferometer used for phase-sensitive detection of fs nonresonant Raman experiments is illustrated in Figure 1(c). Following the polarizers, each beam was focused with a 50 cm lens to a 250 μm spot on an DO optimized for 633 nm. The beams were spatially crossed in the horizontal plane at an angle of $\sim$3°. The +1 and −1 orders from each pulse, diffracted in the vertical plane at angles of 2.4°, were imaged into the sample using the familiar "box car" geometry shown in Figure 1(b). The transmission efficiency for each pulse from the DO to the pair of pulses at the sample was $\sim$52%. The total energy of the three input pulses incident on the sample was 0.4 μJ and 0.8 μJ for the CS_2 and CH_3CN measurements, respectively.

Note that the interferometer used reflective optics instead of lenses to minimize pulse distortion. A 25 cm spherical mirror and a flat folding mirror were used for the lenses L2 and L3 shown schematically in Figure 1(c). The pulses were imaged achromatically onto the sample cell by a concave mirror placed one radius away from the DO1 and the sample. The curved mirror was tilted off-axis horizontally by 4° onto the folding mirror. Alignment in the horizontal dimension throughout the interferometer was flat to ensure no variation of timing between the pulse pairs. Masks ensured that only three beams were allowed to focus onto the sample ($\mathbf{E_1}$, $\mathbf{E_2}$, and $\mathbf{E_3}$). Following the phase-matched geometry, the signal was radiated into the $\mathbf{k_4}$ direction (see Figure 1(b)). The two pump beams were blocked after the sample while the signal and the probe beam ($\mathbf{E_3}$), acting as the local oscillator $\mathbf{E}_{LO}$, were recombined on DO2. The imaging of the LO and the signal beams after the sample was done using a second folding mirror and a 25 cm concave mirror placed one radius away from both the sample and DO2. This ensured the spatial and temporal overlap of the LO and the signal field allowing for true heterodyne detection of the signal field. The ratio of the signal amplitude to that of the LO was less than 2%, which allowed us to ignore the homodyne signal contribution as shown in eq 6. The spot corresponding to the overlap of the +1 and −1 diffraction orders of the two beams was sent through an analyzing polarizer to a silicon photodiode. The signal beam was chopped at 500 Hz before being recombined with the LO, and a lock-in amplifier was used to detect the transient grating signal.

The relative phase between the LO and the signal beam, ϕ, was adjusted by varying the delay of the LO pulse envelope relative to the signal. A microscope cover slip of thickness $\sim$150 μm was split into two, and each half was placed in the path of the signal and LO beams after the sample. Rotation of the cover slip by 8° in the LO arm allowed the phase difference between the two arms to be varied by $\pm\pi$ with resolution of 0.25°. Destructive interference fringes were characterized by almost complete extinction of the beam over the entire mode after the second DO. The phase difference (ϕ) was calibrated by taking an interference pattern between the two probe beams with the pump beam blocked. The intensity of the interferogram was modulated by >85%. If longer delays are introduced, for instance with a thicker cover slip, this interferogram will allow the absolute phase difference between the two arms to be determined.

This method of passive phase locking exhibited phase drifts of ±10° over a 2-h period. Calibrations were checked before and after each scan to ensure no significant drift during data acquisition. The phase drift in this two-diffractive-optic interferometer arises from minor path length differences between the signal and the LO, and precise alignment of the two beams in the horizontal and vertical dimensions can reduce it. Using the same microscope cover slip for both the signal and LO to ensure that both the beams travel through the same amount of glass is crucial to the phase stability of this technique.

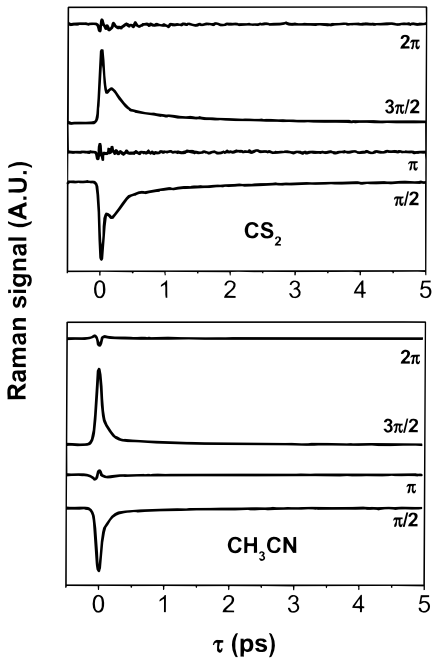

Figure 2. Phase-sensitive detection of the third-order polarization in CS_2 (top panel) and CH_3CN (bottom panel) for the R_{ZZZZ} tensor element. The four traces in each panel were collected for different relative phases between the probe and LO. The total energy of the three input pulses ($\mathbf{E_1} + \mathbf{E_2} + \mathbf{E_3}$) incident on the sample was 0.4 μJ and 0.8 μJ for the CS_2 and CH_3CN measurements, respectively.

Nonresonant experiments were performed on CS_2 (>99.9%) and CH_3CN (>99.9%) contained in a static 1 mm path length fused silica cuvette. Polarization-selective measurements were made by rotating the angle of the pump polarizer (θ_{pump}), while the angles of the probe polarizer (θ_{probe}) and the analyzer (θ_{anal}) were kept constant at 0°.

Results and Discussion

Figure 2 demonstrates the phase-sensitive detection of the nonresonant response from liquid CS_2 and CH_3CN for LO phase angles, ϕ, between $\pi/2$ and 2π. As expected for transparent liquids, the birefringent response, detected when the induced phase shift is in odd multiples of $\pi/2$, is appreciably greater than the dichroic response, observed for even multiples of $\pi/2$.[12] Our studies indicate that the amplitude of the dichroic response is ≤12% of the birefringent response. The only significant contribution to the dichroic responses occurs near $\tau = 0$, at which point near-resonant two-photon electronic processes may contribute.

While more effort is required to align the dual DO interferometer, there are a number of advances of this experimental method over other OHD-TG experiments employing a single DO.[18,19,21,24,25] A two-DO interferometer allows the absolute phase shift between the LO and signal arms to be accurately calibrated, and no assumptions need to be made regarding the magnitude of the birefringent and dichroic responses in transparent liquids.

Another advantage is that only three fundamental beams are incident on the sample, so that only the signal of interest is radiated along the wave vector matched direction $\mathbf{k_S} = \mathbf{k_1} - \mathbf{k_2}$

$+ \mathbf{k_3}$. Chopping the signal beam before recombining the signal and the LO in the second DO ensures that the TG signal is not mixed with any two-pulse, pump−probe (PP) signals. To elaborate on this issue, consider the signal contributions when all four beams ($\mathbf{E_1}$, $\mathbf{E_2}$, $\mathbf{E_3}$, and $\mathbf{E_4}$) are focused onto the ,sample and the TG signal is detected directly along $\mathbf{k_4}$ ($\mathbf{k_S}$). In this case, $\mathbf{E_4}$ acts as the LO for an OHD scheme. Neglecting the polarization states of the beams, four third-order signals, originating from different input wave vector permutations, are radiated along this wave vector matched direction $\mathbf{k_4}$: $\mathbf{E_s}(\tau, \mathbf{k_S} = \mathbf{k_1} - \mathbf{k_2} + \mathbf{k_3})$, $\mathbf{PP_4}'(\tau, \mathbf{k_4} = \mathbf{k_1} - \mathbf{k_1} + \mathbf{k_4})$, $\mathbf{PP_4}''(\tau, \mathbf{k_4} = \mathbf{k_2} - \mathbf{k_2} + \mathbf{k_4})$, and $\mathbf{PP_4}'''(\tau = 0, \mathbf{k_4} = \mathbf{k_3} - \mathbf{k_3} + \mathbf{k_4})$. $\mathbf{E_s}(\tau)$ is the transient grating signal of interest, which is composed of birefringent and dichroic responses while the three pump−probe ($\mathbf{PP_4}$) signals are caused by the pump-induced birefringence in the sample generated along $\mathbf{k_4}$. Two interactions with the pump beams ($\mathbf{k_1}$ or $\mathbf{k_2}$) and one interaction with the probe ($\mathbf{k_4}$) generate the third-order nonlinear PP signals. The PP signals are radiated along the probe direction, and therefore the probe serves as an in-quadrature LO for heterodyne detection. These pump−probe signals are of the same magnitude and follow the same dynamics as the TG signals. The probe beam serves as a LO for the signal(s) emitted by the third-order polarization in its phase-matched direction $\mathbf{k_4}$. Notice that $\mathbf{PP_4}'''$ has no time dependence, but will presumably have mixed birefringent and dichroic character that we observe near $\tau = 0$. It is important that these pump−probe signals ($\mathbf{PP_4}'(\tau)$, $\mathbf{PP_4}''(\tau)$ and $\mathbf{PP_4}'''(0)$) be distinguished from the TG signal in four-wave mixing experiments, particularly when variable polarization states for the two pump beams are used.

The two-DO method offers a reliable method of making sure that the TG signal is not contaminated with these extra signals. Only three beams are focused onto the sample cell, namely $\mathbf{E_1}$, $\mathbf{E_2}$, and $\mathbf{E_3}$. The TG signal, generated in the $\mathbf{k_4}$ direction is given by $\mathbf{E_s}(\tau)$, and $\mathbf{E_3}$ serves as the LO after the sample. Two pump−probe signals are radiated along $\mathbf{k_3}$: $\mathbf{PP_3}'(\tau, \mathbf{k_3} = \mathbf{k_1} - \mathbf{k_1} + \mathbf{k_3})$ and $\mathbf{PP_3}''(\tau, \mathbf{k_3} = \mathbf{k_2} - \mathbf{k_2} + \mathbf{k_3})$. The detector sees a sum of the LO, the TG signal and the PP signals radiated along $\mathbf{k_3}$, indicated below by the summation over the index i

$$I(\tau,\phi) = \frac{nc}{4\pi}|\mathbf{E}_{LO}(\tau,\phi) + \mathbf{E}_s(\tau) + \sum_i PP_{3i}\cos(\omega\tau + \phi)|^2 \quad (7)$$

To remove any pump−probe artifacts along the LO path, we chop the signal prior to recombining. In the limit that $\mathbf{E_{LO}} \gg \mathbf{E_s}(\tau)$ ($E_{bir} + E_{dic}$), $\mathbf{PP_3}'(\tau)$, and $\mathbf{PP_3}''(\tau)$, only the desired signal is detected. This intense LO limit is readily achieved by controlling the intensity of the input beams. The final result is the same as that of eq 5, allowing the birefringent and dichroic signals to be distinguished from competing pump−probe contributions.

A phase-sensitive measurement technique allows phase-cycling methods for data acquisition to be designed. NMR spectroscopy has taken advantage of quadrature detection to remove artifacts, correct for baseline drift and pulse imperfections, and select particular responses from two-dimensional spectra. Phase-cycling of the LO in detection of fs optical signals can be used for the same purposes.[26] In OHD−OKE spectroscopy, subtraction of two scans with an LO introduced by tilting the probe polarizer away from extinction by both positive and negative angles has previously been used to remove homodyne signal contributions.[27] Analogously, we can remove pump−probe contributions, homodyne signals, and baseline imperfections by subtracting two data scans with a π-phase-shifted LO between scans. This principle becomes particularly important in the development of two-dimensional nonresonant techniques. Phase cycling in fifth-order Raman spectroscopy has the potential to remove unwanted cascading signal contributions. Cascading nonlinearities are emitted out of phase with the direct nonlinear signals, suggesting that phase cycling can be used to separate these contributions.[28,29] It should further be pointed out that this method is not limited to nonresonant experiments.[24,25] The methods of phase-cycling will allow signal dichroic and birefringent contributions in resonant experiments to be separated without interference from pump-induced modulation of the LO field.

Along with the phase-sensitive detection, a nonresonant TG allows for polarization control over the pump and probe beams for studying liquid dynamics. In an isotropic liquid, there are four nonzero tensor elements of the molecular polarizability tensor: R_{ZZYY}, R_{ZYZY}, R_{ZYYZ}, and R_{ZZZZ}. These four nonzero elements are related to each other by $R_{ZZZZ} = R_{ZZYY} + R_{ZYZY} + R_{ZYYZ}$.[30] In addition, $R_{ZYZY} = R_{ZYYZ}$ for nonresonant experiments, implying that the measurement of R_{ZZYY} and R_{ZZZZ} completely describes the nuclear polarizability relaxation dynamics of the group state in isotropic systems. The more appropriate basis set of response functions for extracting information about liquid dynamics in these third-order nonlinear experiments is the anisotropic and isotropic responses. OHD−OKE and OHD−RIKES[6−10,27,31] experiments are selective only to the anisotropic response for various systems.

$$R_{ANISO} = R_{ZZZZ} - R_{ZZYY} = R_{ZYYZ} + R_{ZYZY} \quad (8)$$

Yet until this time, the isotropic response in liquids, which suppresses reorientational dynamics, has been largely neglected

$$R_{ISO} = R_{ZZZZ} + 2R_{ZZYY} \quad (9)$$

By suppressing reorientational motion, R_{ISO} is sensitive to interaction-induced effects and may be used to gain insight into density fluctuations of the liquid.

R_{ZZZZ} is measured by setting the input polarizers and analyzer parallel ($\theta_{pump} = \theta_{probe} = \theta_{anal} = 0°$), whereas R_{ZZYY} is measured by crossing the polarization of the pump pulses with the probe and analyzer ($\theta_{pump} = 90°$; $\theta_{probe} = \theta_{anal} = 0°$). R_{ISO} is measured directly by probing and detecting at the magic angle ($\theta_{MA} = 54.7°$) relative to two parallel-polarized pump beams. While, R_{ISO} can be measured directly, we can calculate R_{ANISO} using R_{ZZZZ} and R_{ZZYY} (eq 8).

Figure 3 shows polarization-selective measurements of the birefringent response of CS_2. The three traces in the top panel show the experimentally measured time-dependent response functions corresponding to R_{ZZZZ}, R_{ZZYY}, and R_{ISO}. The traces corresponding to the R_{ZZZZ} and R_{ZZYY} geometries agree with previous measurements of these response functions using TG[16−19,21] and positive Kerr lens[32,33] methods. It is observed that R_{ZZZZ} and R_{ZZYY} traces exhibit the characteristic CS_2 behavior, with the inertial intermolecular response peaking at 170 fs and then damping toward an exponential 1.6 ps decay for $\tau >$ 2ps attributed to reorientational dynamics.[8] The lower panel shows a semilog plot of R_{ANISO} obtained from eq 7 and the measured R_{ISO}. The important observation is the stark difference between the anisotropic and the isotropic dynamics. While the long time dynamics of R_{ANISO} are exponential, the isotropic dynamics damp rapidly in a nonexponential manner. A qualitative examination of the two traces suggests that relaxation at early time results from a combination of isotropic dynamics arising from interaction-induced effects (dipole−

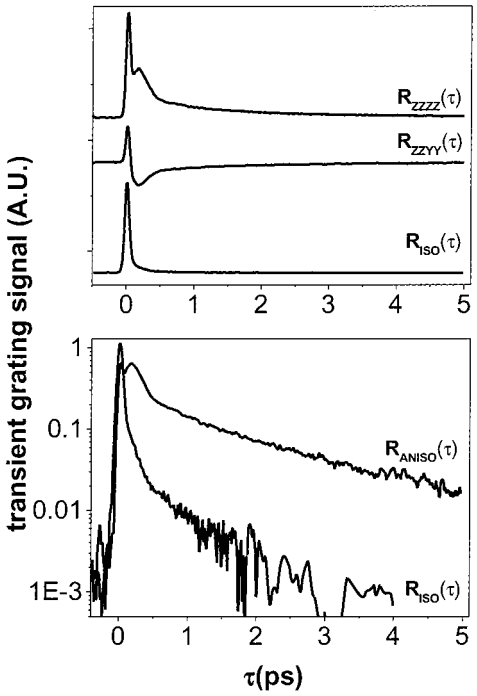

Figure 3. Variable polarization measurements of the intermolecular polarizability relaxation of CS_2 using phase-sensitive detection. All traces are for the birefringent response ($\phi = \pi/2$). The three traces in the top panel represent the time-dependent response functions $R_{ZZZZ}(\theta_{pump} = 0°)$, $R_{ZZYY}(\theta_{pump} = 90°)$ and $R_{ISO}(\theta_{pump} = 54.7°)$, respectively. Note that $\theta_{probe} = \theta_{anal} = 0°$ for all of the polarization-selective studies. The bottom panel shows a semilog plot of the experimentally measured R_{ISO} and the calculated trace of $R_{ANISO} = R_{ZZZZ} - R_{ZZYY}$.

induced dipole interactions) and anisotropic dynamics (primarily librational),[34,35] but it is dominated by diffusive reorientational motion at later times. A more complete analysis will be given elsewhere.

Conclusion

We have demonstrated phase-sensitive detection of polarization-selective TG experiments using a dual diffractive optic arrangement. This approach separates the TG signal from competing pump−probe signals and allows for accurate control of the relative phase between the LO and probe fields without the added complexity of active phase locking. Nonresonant experiments on relaxation dynamics of collective modes in CS_2 and CH_3CN demonstrate that the magnitude of the birefringent response exceeds that of the dichroic response by an order of magnitude. Using the TG method, independent elements of the fourth-rank polarizability tensor can be measured. We also reported the direct measurement of the isotropic collective relaxation dynamics of CS_2, which suppresses reorientational motion to observe interaction-induced effects. Polarization and phase sensitive measurements such as these can clearly be used to separate contributions of molecular relaxation mechanisms to the collective molecular dynamics of liquids. While previous experiments have demonstrated polarization selectivity and/or heterodyning capabilities, this method allows both of these capabilities with the additional discrimination against contaminating pump−probe signals.

Acknowledgment. We thank Prof. Keith Nelson for many helpful discussions. This work was supported by the National Science Foundation (CHE-9900342). Additional support was provided by the Division of Chemical Sciences, Office of Basic Energy Sciences, U.S. Department of Energy (DE-FG02-99ER14988).

References and Notes

(1) Gordon, R. J.; Rice, S. A. *Annu. Rev. Phys. Chem.* **1997**, *48*, 601.
(2) Dhar, L.; Rogers, J. A.; Nelson, K. A. *Chem. Rev.* **1994**, *94*, 157.
(3) deBoeij, W. P.; Pshenichnikov, M. S.; Wiersma, D. A. *Annu. Rev. Phys. Chem.* **1998**, *49*, 99.
(4) Tokmakoff, A.; Lang, M. J.; Larsen, D. S.; Fleming, G. R. *Chem. Phys. Lett.* **1997**, *272*, 48.
(5) Gallagher, S. M.; Albrecht, A. W.; Hybl, J. D.; Landin, B. L.; Rajaram, B.; Jonas, D. M. *J. Opt. Soc. Am. B* **1998**, *15*, 2338.
(6) Cho, M.; Du, M.; Scherer, N. F.; Fleming, G. R.; Mukamel, S. *J. Chem. Phys.* **1993**, *99*, 2410.
(7) Deuel, H. P.; Cong, P.; Simon, J. D. *J. Phys. Chem.* **1994**, *98*, 12600.
(8) McMorrow, D.; Thantu, N.; Melinger, J. S.; Kim, S. K.; Lotshaw, W. T. *J. Phys. Chem.* **1996**, *100*, 10389.
(9) Smith, N. A.; Meech, S. R. *Faraday Dsicuss.* **1997**, *108*, 35.
(10) Feldstein, J. J.; Vöhringer, P.; Scherer, N. F. *J. Opt. Soc. Am. B* **1995**, *12*, 1500.
(11) Scherer, N. F.; Ziegler, L. D.; Fleming, G. R. *J. Chem. Phys.* **1992**, *96*, 5544.
(12) Ziegler, L. D.; Fan, R.; Desrosiers, A. E.; Scherer, N. F. *J. Chem. Phys.* **1994**, *100*, 1823.
(13) Cho, M.; Fleming, G. R.; Mukamel, S. *J. Chem. Phys.* **1993**, *98*, 5314.
(14) Eesley, G. L.; Levenson, M. D.; Tolles, W. M. *IEEE J. Quantum Elect.* **1978**, *QE−14*, 45.
(15) Vöhringer, P.; Scherer, N. F. *J. Phys. Chem.* **1995**, *99*, 2684.
(16) Chang, Y. J.; Cong, P.; Simon, J. D. *J. Phys. Chem.* **1995**, *99*, 7857.
(17) Matsuo, S.; Tahara, T. *Chem. Phys. Lett.* **1997**, *264*, 636.
(18) Goodno, G. D.; Dadusc, G.; Miller, R. J. D. *J. Opt. Soc. Am. B* **1998**, *15*, 1791.
(19) Goodno, G. D.; Astinov, V.; Miller, R. J. D. In *Ultrafast Phenomena IX*; Springer-Verlag: Berlin, 1998.
(20) Maznev, A. A.; Crimmins, T. F.; Nelson, K. A. *Opt. Lett.* **1998**, *23*, 1378.
(21) Maznev, A. A.; Nelson, K. A.; Rogers, J. A. *Opt. Lett.* **1998**, *23*, 1319.
(22) Mukamel, S. *Principles of Nonlinear Optical Spectroscopy*; Oxford University Press: New York, 1995.
(23) Khalil, M.; Golonzka, O.; Demirdöven, N.; Fecko, C.; Tokmakoff, A. *Chem. Phys. Lett.* **2000**, *321*, 231.
(24) Dadusc, G.; Goodno, G.; Chiu, H.; Ogilvie, J.; Miller, R. J. D. *Isr. J. Chem.* **1998**, *38*, 191.
(25) Goodno, G. D.; Astinov, V.; Miller, R. J. D. *J. Phys. Chem. B* **1999**, *103*, 603.
(26) Hinze, G.; Francis, R. S.; Fayer, M. D. *J. Chem. Phys.* **1999**, *111*, 2710.
(27) McMorrow, D.; Lotshaw, W. T.; Kenney-Wallace, G. A. *IEEE J. Quantum Electron.* **1988**, *QE−24*, 443.
(28) Blank, D.; Kaufman, L. J.; Fleming, G. R. *J. Chem. Phys.* **1999**, *111*, 3105.
(29) Cho, M. H.; Blank, D. A.; Sung, J.; Park, K.; Hahn, S.; Fleming, G. R. *J. Chem. Phys.* **1999**, *112*, 2082.
(30) Butcher, P. N.; Cotter, D. *The Elements of Nonlinear Optics*; Cambridge University Press: Cambridge, 1990.
(31) Chang, Y. J.; Castner, E. W., Jr. *J. Phys. Chem.* **1996**, *100*, 3330.
(32) Chang, Y. J.; Cong, P.; Simon, J. D. *J. Chem. Phys.* **1997**, *106*, 8639−8649.
(33) Cong, P.; Chang, Y. J.; Simon, J. D. *J. Phys. Chem.* **1996**, *100*, 8613.
(34) Murry, R. L.; Fourkas, J. T.; Li, W. X.; Keyes, T. *Phys. Rev. Lett.* **1999**, *83*, 3550.
(35) Murry, R. L.; Fourkas, J. T.; Keyes, T. *J. Chem. Phys.* **1998**, *109*, 2814.